JOURNAL OF CATALYSIS 64, 272–283 (1980)

The Kinetics of Methanation on Nickel Catalysts

SA VAN HO AND PETER HARRIOTT

Chemical Engineering Department, Cornell University, Ithaca, New York 14850

Received June 28, 1979; revised January 29, 1980

The kinetics of methanation of carbon monoxide were studied with 2% Ni/SiO_2 and 10% Ni/SiO_2 catalysts in a differential reactor. The role of carbon as an intermediate was explored by making transient tests of carbon deposition, carbon gasification, and methane formation. If carbon is an intermediate, neither the normal dissociation of CO nor reactions of H with C seem to be controlling. The limiting step may be the surface reaction between adsorbed carbon monoxide and hydrogen atoms to form carbon and water. The data suggest surface heterogeneity with over a 10 fold range in activity for adsorbed CO.

INTRODUCTION

Methanation has been used for many years to remove traces of CO and CO_2 from hydrogen-rich gases such as those used for ammonia synthesis. Recent interest is primarily in the methanation of CO as a final step in the production of SNG (substitute natural gas) from coal or other fuels. The feed to the methanator in this case will probably have a moderate amount of CH_4 and a nearly stoichiometric ratio of H_2/CO (3/1). The reaction can be carried out on nickel catalysts at 200 to 400°C and at pressures up to 100 atm. The reaction is almost irreversible under these conditions, but the large heat of reaction ($-\Delta H$ = 50 kcal/mole at 200°C) has complicated some kinetic studies and is a major problem in the design of commercial reactors.

Many empirical correlations and mechanisms proposed for the methanation reaction are reviewed by Vlasenko and Yuzefovich (*1*), Mills and Steffgen (*2*), and Vannice (*3*). The mechanisms can be divided into two major categories: one involves the formation of a CH_nO complex (or complexes) on the catalyst surface, and the other, more prominent in recent work, considers carbon, formed by dissociation of CO, as the important intermediate. Some of the evidence for each type is reviewed below.

Studies of coadsorption of CO and H_2 on nickel catalysts have shown interactions that suggest complex formation. Vlasenko *et al.* (*4*) found that twice as much H_2 adsorbed on a monolayer of CO as on the clean nickel surface, and they proposed a CH_2O complex. Further work (*5*) showed the rate of methanation to be comparable with the rate of complex formation. Wedler *et al.* (*6*) reported that in the presence of preadsorbed H_2, much more CO could be adsorbed than on clean nickel films, indicating that adsorbed hydrogen induces linear adsorption of CO. Horgan and King (*7*) also found that the total moles of H_2 + CO adsorbed exceeded the coverage of either H_2 or CO alone. However, most of the above tests were done at temperatures of 100°C or lower, far from normal methanation conditions.

To get evidence for an intermediate complex at reaction conditions, Farrauto (*8*) used a thermal balance to follow weight changes of $Ni–Al_2O_3$ catalysts. At 100–200°C, the weight gain corresponded to monolayer coverage by COH_n (n = 0, 1, 2, etc.) but more than monolayer coverage if C or CH_n were assumed the dominant species. The weight of adsorbed species de-

0021-9517/80/080272-12$02.00/0

creased by 75% as the temperature increased from 200 to 300°C, but it changed only slightly from 300 to 400°C. This could mean a switch to a lighter complex or desorption of adsorbed CO.

Various models that include intermediate complexes have been postulated to explain the observed reaction orders and activation energies. Vannice (*9*) proposed equilibrium formation of a CHOH complex, with the addition of more hydrogen as the controlling step. McGill and Richardson (*10*) also assumed stepwise addition of H to adsorbed CO, with the slow step changing with temperature to account for a decrease in activation energy and an increase in apparent reaction order of H_2. These and other models in which one step of the surface reaction controls lead to equations of the Langmuir–Hinshelwood type, which predict a sharp maximum in the graph of rate versus CO pressure. Many of the published studies cover only the region where the order for CO is negative, but a few show a long region of zero-order behavior at lower CO pressures or a very broad maximum in the rate curves. To fit this trend, Fontaine and Harriott (*11*) presented a model with two slow steps: the formation of a CH_2O complex from adsorbed CO and H, and the reaction of the complex with H. The model was consistent with the observed gradual decrease in methane production after a step decrease in CO feed.

The use of fundamental adsorption characteristics for CO and H_2 in developing a model for methanation is illustrated by the study of Polizzotti *et al.* (*12*). They concluded that almost all of the nickel surface (99.99% at 230°C) is covered by CO, leaving very few sites for adsorbed H. Their model has two Eley–Rideal steps, with the slow step being reaction of H_2 with a CHO complex, which was formed from adsorbed H plus CO from the gas. This mechanism is not consistent with the transient studies of Fontaine and Harriott (*11*), but it is a promising step in the development of models that allow for the effects of temperature and reaction on surface coverage.

The major problem with models based on a CH_nO complex is that attempts to identify such a complex by infrared-red spectroscopy have not been successful (*13*). However, if the formation of the complex is the slow step, not much would be present on the surface during reaction.

The role of carbon as a possible intermediate in methanation was studied by Araki and Ponec (*4*). Above about 200°C, CO adsorbed on nickel disproportionates to $C + CO_2$, and the carbon on the surface reacts readily with hydrogen to form methane. An increase in the amount of carbon increases the methanation rate, and at less than monolayer coverage, the rate exceeds the rate of the $CO + H_2$ reaction at the same temperature and hydrogen pressure. The authors proposed that hydrogenation of C_s, or CH_s, or $(CH_2)_s$ is the limiting step in methanation of CO in order to explain the observed dependence on hydrogen pressure. However, the high activity of deposited carbon and the slightly lower activation energy for its gasification (17 kcal vs 20–25 for CO methanation) indicate a more complex model is needed if carbon is indeed a key intermediate.

Other workers have reported two different species of carbon on nickel surfaces. Madden and Ertl (*15*) dissociated chemisorbed CO by electron bombardment and followed the removal of CO by thermal desorption. After the unreacted CO left at about 180°C, there was a β_1 peak at 280–380°C, attributed to amorphous carbon reacting with adsorbed oxygen, and a β_2 peak at 530°C, due to graphite clusters reacting with oxygen. McCarty *et al.* (*16*) also found two forms of surface carbon using temperature-programmed desorption in the presence of hydrogen. Carbon in the α-state reacted at about 200°C with an activation energy of 17 kcal. Carbon in the β state had an activation energy of 33 kcal and a peak reaction temperature of 400°C. The α carbon slowly transformed into β carbon with

an activation energy 8 kcal/mol. The α and β states probably correspond to the β_1 and β_2 states of Madden and Ertl.

Wentrcek *et al.* (*17*) found that carbon deposited from Co on a commercial nickel catalyst at 280°C was very active toward H_2. However, when held at 450°C for 10 min, the carbon became very unreactive. This is further evidence that the active carbon is not stable, but transforms into the unreactive form at a rate dependent on temperature.

There are several points that need to be resolved before carbon can be accepted as a key intermediate in the methanation of CO on nickel catalysts. Since the methanation of carbon is much faster than that of CO, the carbon + H reaction is probably not rate limiting, which suggests that dissociation of CO may be the slow step. However, simple dissociation of CO does not involve hydrogen, whereas all workers agree that hydrogen has a positive effect on the methanation rate. Furthermore, the methanation reaction is often negative order to CO, whereas the rate of CO dissociation increases with concentration of CO. Also, the reported activation energies for the disproportionation of CO (33 kcal) and the hydrogenation of deposited carbon (17 kcal) both differ from that for methanation of CO (20–25 kcal), so that neither of the first two processes seems likely to control the rate of the third reaction. However, the reaction orders for H_2 and CO differ for these three reactions, and the apparent activation energies are probably not constant. A comparison of these three reactions would be more meaningful when done over a wide range of temperatures and gas compositions, and that is one of the main objects of this work.

APPARATUS AND PROCEDURE

Kinetic measurements were made using a $\frac{3}{8}$-in.-diam stainless-steel reactor immersed in a fluidized-bed sand bath. The feed gases, He, CO, H_2, and CH_4, were passed through beds of molecular sieves and charcoal adsorbent and metered with rotameters before being combined and sent to a preheater in the sand bath. A three-way valve was used to permit step changes in CO or H_2 concentration. Thermocouples measured the bath and feed temperatures, and a movable axial thermocouple was used to measure temperatures in the catalyst bed.

The product stream was analyzed by gas chromatography, and H_2, CO, CH_4, and CO_2 were separated in 1.5 min by a $\frac{1}{4}$-in.-o.d. × 10-ft stainless-steel column packed with 100- to 200-mesh Poropak Q. The column was kept at 100°C and the thermal conductivity detector at 110°C. The carrier gas was helium (60 cm^3/min), which was dried and purified using molecular sieves and a small bed of nickel catalyst at 300°C.

The water peak had too much tailing for accurate chromatographic analysis, even when the sample lines were heated and the column and detector temperatures raised to 160–170°C. For a few tests, water was determined by passing the product stream through a bed of $CaSO_4$ for a short time to adsorb all of the water. The bed was then heated to 250°C and purged with helium, giving a moderately broad but reproducible pulse at the thermal conductivity detector.

Steady-state methanation tests were made with a continuous feed of H_2, CO, and He, and the CO conversion was less than 10% for most runs. However, the reaction rates were the same up to 50% conversion or higher, so the rate was based on the amount of CH_4 in the product gas, even for runs at high conversion. In a few runs CH_4 was added to test for inhibition effects, and some tests were made at low flow rates to approach complete conversion. The reactor temperature was usually within 1°C of the bath temperature. For the highest temperature runs, the catalyst was mixed with sand to keep the temperature difference below 3°C. The reactor wall and the sand had negligible catalyst activity.

The response of the catalyst to step changes in CO concentration was measured

under reaction conditions to determine the total amount of CO or carbon-containing species on the catalyst surface. Samples were taken about once a minute after the step change, and some runs were repeated to fill in the curves with additional data points. Similar tests were made at about 200°C to determine chemisorbed CO in the absence of H_2; the catalyst was cleaned in H_2 overnight at $T \geqq 300$°C and flushed with purified He for 3–4 hr before exposure to CO. The chemisorption of CO and of H_2 was also measured by the pulse technique.

Carbon was deposited by the disproportionation of CO at 300–350°C. The reaction was studied by suddenly adding CO to a flowing stream of helium and following CO_2 formation with time. Before these runs, the catalyst was cleaned using the same procedure as for CO chemisorption. After forming the desired amount of carbon, the reactor was flushed with helium and cooled to 200–250°C for gasification.

A 10% nickel catalyst was prepared by making a paste of nickel nitrate solution and M-5 Cab-O-Sil. This support consists of clusters of partially sintered particles about 120 Å in diameter. The catalyst was dried, pressed into wafers, and crushed to 28–48 mesh. Reduction was carried out using 30% H_2 in N_2 at temperatures slowly increasing from 200 to 450°C. The reduced catalyst was cooled slowly to room temperature and passivated in a stream of air + N_2. A catalyst with 2% Ni was prepared by mixing the green 10% catalyst with additional silica and following a similar reduction procedure, except that the final reduction temperature was 400°C.

The catalysts were examined by electron microscopy, and the 10% Ni catalyst had crystallites from 50 to 250 Å in size. The 2% catalyst had crystallites from 50 to 180 Å in diameter with most particles about 100 Å.

RESULTS AND DISCUSSION

Steady-State Methanation Tests

The methanation rate was measured for a wide range of carbon monoxide pressures at several temperatures and hydrogen pressures. Figure 1 shows that at 275°C the rate was almost independent of P_{CO} from 0.01 to 0.5 atm. At 255°C, the reaction became negative order to CO at $P_{CO} = 0.05$ atm, and at 212°C, the inhibiting effect of CO was still more pronounced. Data for the 10% Ni catalyst (not plotted) showed that the order with respect to CO changed from strongly negative at 200°C to slightly negative at 247°C and almost zero at 300 and 330°C.

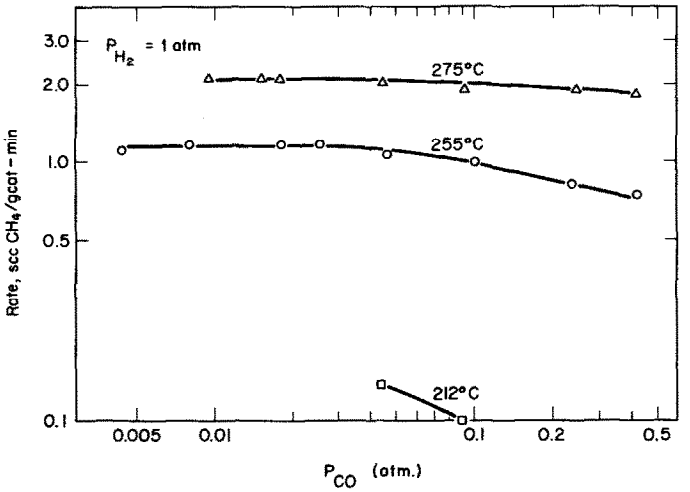

FIG. 1. Effect of P_{CO} on methanation rate for the 2% Ni catalyst.

The reaction rate increased with hydrogen pressure, but the effect changed with gas composition, as shown in Fig. 2. The apparent reaction order for H_2 was 0.6 to 0.8 for $P_{H_2} = 0.2$ to 1.0 atm, but it decreased at higher hydrogen pressure. Also, the reaction order for CO, which was negative at low value of P_{H_2}, became positive at $P_{H_2} = 3.0$ atm. These results suggest competitive adsorption of CO and H_2; CO is more strongly adsorbed but may be displaced at high hydrogen pressures.

The apparent activation energies ranged from 25 to 20 kcal, and both catalysts had slightly lower values at the higher temperatures, as shown in Fig. 3. This slight decrease probably reflects the fact that CO inhibition at a given value of P_{CO} becomes less as the temperature is increased. Originally, the 2% catalyst was more active than the 10% catalyst per gram of nickel, but the 2% catalyst was partially deactivated by exposure to impure CO_2 or by treatment under severe conditions of temperature and carbon deposition. During methanation tests, the catalyst showed no further aging, and the low activity permitted tests at temperatures up to 400°C. The runs at 300–400°C were made with catalyst crushed to 0.2 mm to minimize pore diffusion effects. The falloff in rate at the highest temperature is not a mass transfer effect, since comparable absolute rates were obtained with the 10% catalyst at 300°C with no evidence of a break in the graphs.

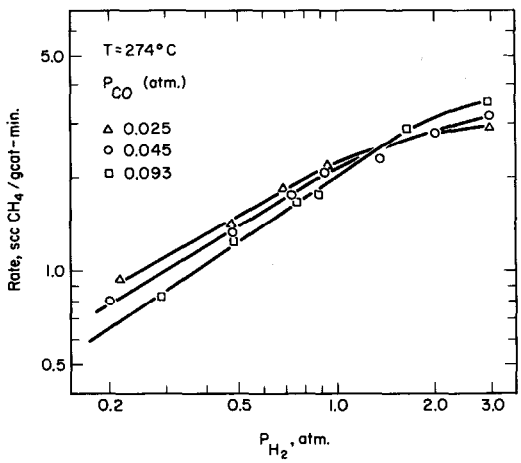

FIG. 2. Effect of P_{H_2} on methanation rate for the 2% Ni catalyst.

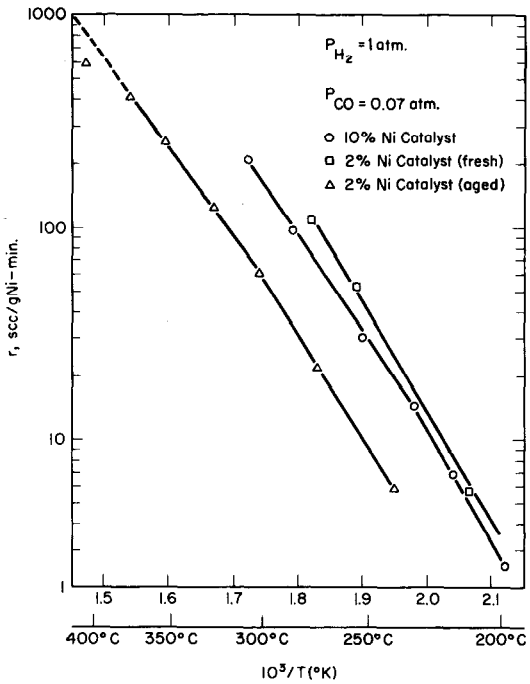

FIG. 3. Comparison of methanation activities for the two catalysts.

Runs at high CO conversions showed practically constant rates at 215 and 230°C when a large excess of H_2 was present. At 300 and 300°C, similar tests showed a slight decrease in rate as 100% conversion was approached (Fig. 4). At these temperatures some CO_2 was formed, and the amount was greater when the hydrogen concentration was lowered to the stoichiometric value. The CO_2 may be formed by the water–gas shift reaction, which becomes more important only after appreciable accumulation of water in the product gas:

$$CO + 3H_2 \rightarrow CH_4 + H_2O \qquad (1)$$

$$CO + H_2O \rightleftharpoons CO_2 + H_2. \qquad (2)$$

Transient Response Experiments

The change in gas composition at the reactor outlet following a step increase in

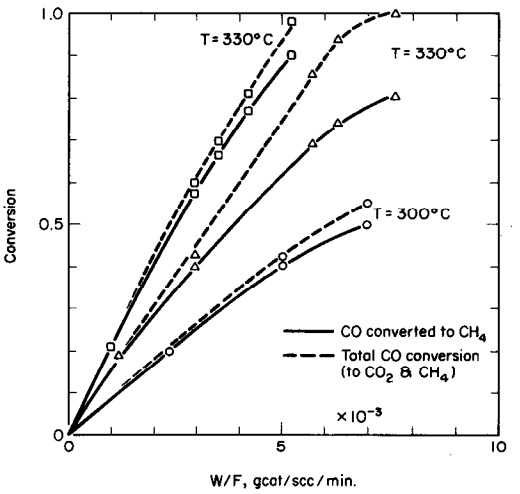

FIG. 4. Effects of CO conversion on the rate and the selectivity of methane formation for the 10% Ni catalyst. (○, △) Feed: 72% He, 21% H_2, 7% CO; (□) Feed: 50% He, 43% H_2, 7% CO. P_T = 1 atm.

P_{CO} is shown in Fig. 5. The data are corrected for the holdup time in the system. The methane concentration increased almost linearly with time to a maximum and then decreased slightly to a steady-state value. Carbon monoxide did not appear for 3 min, and then its concentration rose rapidly to a final value. The total CO taken up by 6 g of fresh catalyst in the presence of H_2 was 17 cm^3; after the catalyst had been used for 2 weeks or more, similar tests gave 15.5 cm^3 adsorbed at 195°C.

For the same catalyst at about the same temperature (195°C) only 13 cm^3 of CO was adsorbed in the absence of H_2. The amount adsorbed was the same for P_{CO} = 0.02 to 0.10 atm, but decreased to 11 cm^3 at P_{CO} = 0.007 atm. The maximum chemisorption from helium was about 15% less than the amount on the surface during reaction with hydrogen. The enhanced adsorption of CO in the presence of H_2 is consistent with earlier studies by Wedler *et al.* (*18*) and Horgan and King (*7*) and may be caused by a shift from the bridged to the linear mode of adsorption. The amount of CO taken up indicates clearly that CO, or a carbon-containing species, covered most of the surface sites under methanation conditions.

The response to a step decrease in CO concentration reveals more about the nature of the reaction. After turning off the CO in the feed, the CH_4 concentration rose quickly to a maximum and gradually decreased during the next 10 min. With a higher initial value of P_{CO} and a lower steady-state rate, the increase in CH_4 was more dramatic, as shown in Fig. 6. However, all of the curves had about the same peak value. These results are strong evidence for a reaction between adsorbed CO and adsorbed H_2 or H. At steady state, most of the sites must be occupied by CO or a carbon species, and uncovering a small fraction of these by forming CH_4 greatly increases the sites available for H_2 chemisorption. The increase in H coverage more than offsets the slight decrease in CO coverage, leading to a rate maximum. If hydrogen reacted from the gas phase, the rate

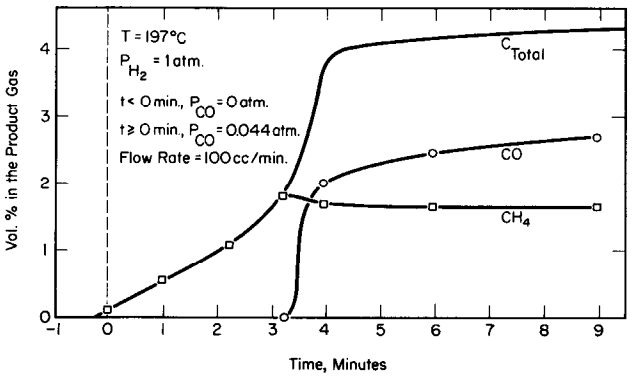

FIG. 5. Response of the 10% Ni catalyst to a step increase in P_{CO}.

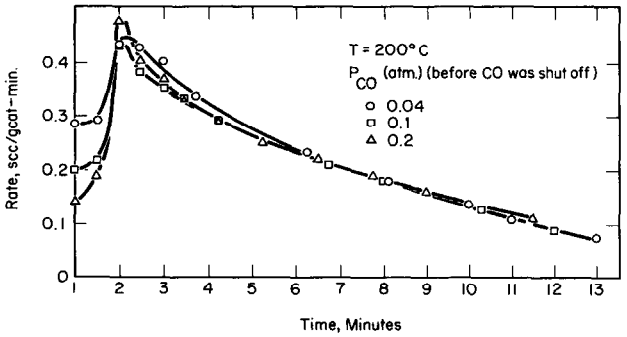

FIG. 6. Responses of the 10% Ni catalyst to a step decrease in P_{CO}.

would gradually decline after shutting off CO, and if CO in the gas played a major role, the rate would drop to zero as soon as CO was swept out of the system.

Curves similar to those of Fig. 6 were obtained at different hydrogen pressures, and the maximum rates are plotted in Fig. 7. Note that the maximum rate increases with the 0.4 power of the hydrogen pressure, about half the order found in steady-state tests on the same catalyst. This difference and the shape of the curves in Fig. 6 will be treated later in the discussion of reaction mechanisms.

The amount of H_2O removed from the catalyst after a step decrease in CO was measured to see if the species on the surface contained oxygen. For three runs at 230°C and $P_{CO} \cong 0.05$ atm, the molar ratio of H_2O/CH_4 collected was 0.6 to 0.7, indicating appreciable coverage by CO or a CH_nO complex, rather than by carbon. The oxygen is probably not present as O_s, since this species reacts very rapidly with CO or with H_2. The variation in H_2O recovery with gas composition and temperature was not studied.

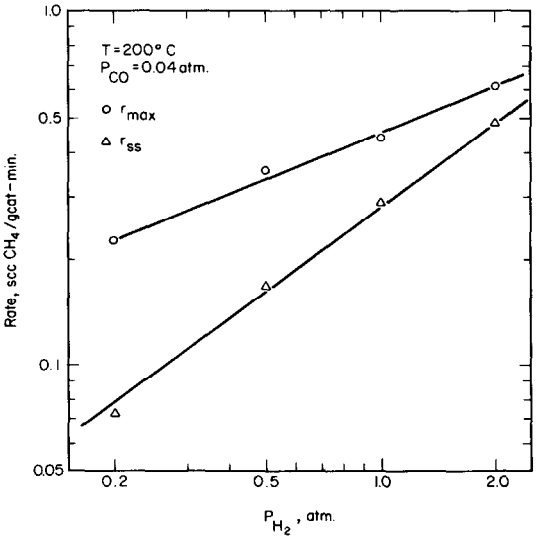

FIG. 7. Effect of P_{H_2} on steady-state and maximum methanation rates for the 10% Ni catalyst.

Carbon Deposition

Carbon was deposited on the catalyst by the disproportionation of CO at 300 to 350°C:

$$2CO \rightarrow C + CO_2. \quad (3)$$

The reaction probably takes place in two steps:

$$CO_s \rightarrow C_s + O_s \quad (4)$$

$$CO_s \text{ (or } CO_g) + O_s \rightarrow CO_2. \quad (5)$$

Subsequent tests showed that the reaction of preadsorbed oxygen with carbon monoxide is very rapid, so there is probably little oxygen on the surface during the disproportionation reaction, and the CO_2 released can be taken as a measure of the carbon formed.

Typical carbon deposition data are shown in Fig. 8. The rate of CO_2 formation rose quickly to a maximum and then declined to a nearly constant value after about 6 min. At 330°C, exposure to CO for 10 min

deposited an amount of carbon equivalent to a monolayer, but the rate decreased only slightly with time, and carbon could still be deposited after 1 hr. The maximum rate and the pseudo-steady-state rate varied with $(P_{CO})^{0.4}$, and the activation energies for carbon deposition were 10–12 kcal for the 2% Ni catalyst (Fig. 10) and 14 kcal for the 10% Ni catalyst (Fig. (11). These values are much lower than the 33 kcal reported by Tottrup (*19*) for carbon deposition on Ni–Al_2O_3. However, he measured the rates when amounts of carbon equivalent to about 20 monolayers had been deposited, in contrast to the small amounts present in this work.

Carbon Gasification

Carbon formed from CO was gasified by reaction with H_2, and typical data are shown in Fig. 9.

$$C + 2H_2 \rightarrow CH_4. \qquad (6)$$

The curves were extrapolated to zero time to get the initial rates. The activation energy was about 15 kcal for the 2% Ni catalyst and 9 kcal for the 10% Ni catalyst. Both values were clearly lower than the 20–24 kcal found for methanation of CO. The order with respect to H_2 varied from about

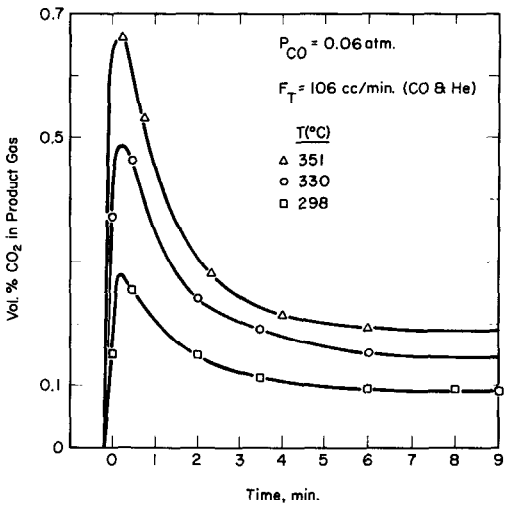

FIG. 8. Rates of carbon deposition over the 2% Ni catalyst.

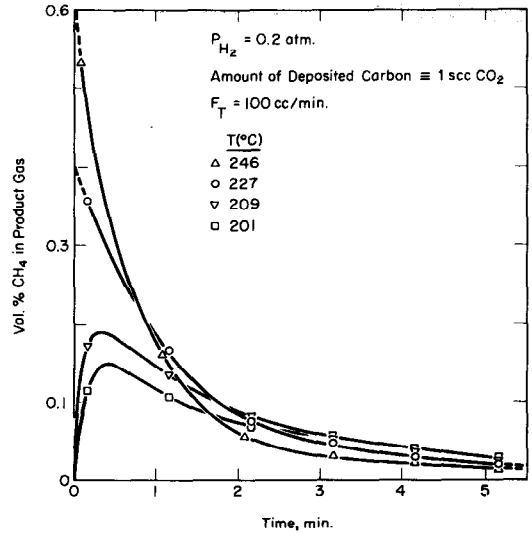

FIG. 9. Rates of carbon gasification over the 2% Ni catalyst.

0.5 at 225°C for the 2% Ni catalyst to only 0.1 at 130°C for the 10% Ni catalyst. The latter was so active that the temperature had to be lowered to measure the carbon activity.

For coverages less than one-third of a monolayer, the gasification rate was proportional to the amount of carbon, but further amounts did not raise the rate proportionately, probably because not all of the carbon was in contact with the catalyst surface. The total amount of carbon obtained as CH_4 was always less than the amount deposited. The fraction that could be easily removed decreased as the amount deposited increased or when the carbon was held in inert gas at 300°C. Table 1 shows some of these results for the 10% Ni catalyst, which had a "monolayer" coverage of 7.5 cm^3 based on CO chemisorption.

Comparison of Methanation, Carbon Deposition, and Carbon Gasification

To clarify the possible roles of carbon deposition and gasification, the rates for these steps are compared with the steady-state methanation rate in Figs. 10 and 11. The data were adjusted to $P_{H_2} = 1.0$ atm and $P_{CO} \cong 0.05$ atm for Fig. 10 and to $P_{H_2} =$

TABLE 1

Some Characteristics of Carbon Deposited on 10% Ni Catalyst

Run	$V_{dep.}$[a] (cm^3)	t at 300°C[b] (hr)	r_i[c] ($cm^3/g \cdot min$)	$V_{gas.}$[d] (cm^3)	$\frac{V_{gas.}}{V_{dep.}}$	r_{CH_4}[e] ($cm^3/g \cdot min$)
1	6.8	0	0.63	3.6	0.53	0.45
2	6.8	1	0.13	2.0	0.29	0.38
3	6.8	0.5	0.64	3.6	0.53	0.34
4	3.4	0	0.41	2.7	0.79	0.36
5	2.6	0	0.33	2.3	0.88	0.36

[a] $cm^3 CO_2$ formed (STP) (7.5 = monolayer).
[b] Time between deposition and gasification.
[c] Initial gasification rate at 170°C, $P_{H_2} = 0.2$ atm.
[d] Total CH_4 formed at 170°C followed by 200°C, $P_{H_2} = 1.0$ atm.
[e] Methanation rate at 204°C, $P_{CO} = 0.02$ atm, $P_{H_2} = 1.0$ atm, measured after gasification test.

0.43 atm for Fig. 11. The maximum rate of carbon deposition was much lower than the methanation rate, and the difference was larger at higher temperatures. If carbon is an intermediate in methanation, some step other than simple dissociation of CO must be involved.

The carbon gasification rates in Fig. 10 are for $\frac{1}{3}$ of a monolayer, and those in Fig. 11 are for 0.9 of a monolayer (equivalent amounts). The initial rate of carbon gasification was much faster than the methanation reaction, showing that if carbon is an intermediate, only a small fraction of the surface need be covered by carbon in order that gasification keep up with the other steps. As the temperature increases, the

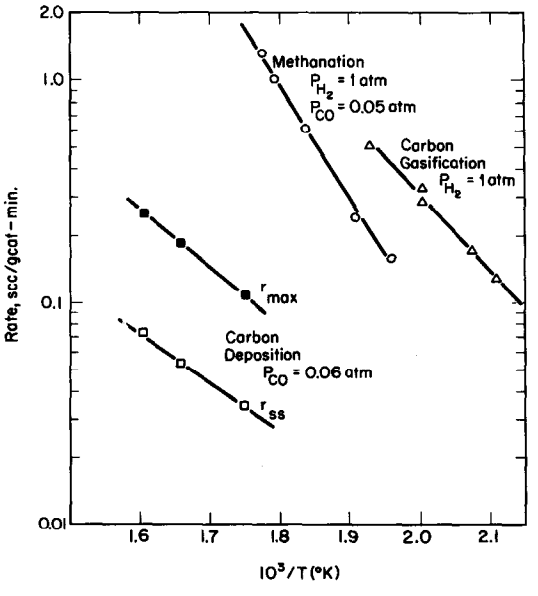

FIG. 10. Comparison of the methanation rates with the rates of carbon deposition and carbon gasification for the 2% Ni catalyst.

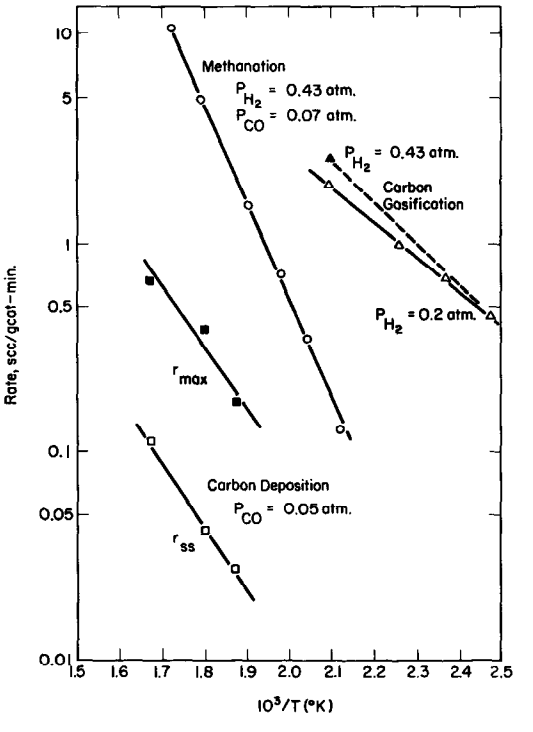

FIG. 11. Comparison of the methanation rate with the rates of carbon deposition and carbon gasification for the 10% Ni catalyst.

difference between the maximum gasification rate and the methanation rate decreases, and perhaps at some temperature, gasification of the carbon would become the limiting step. However, such a temperature cannot be calculated just by extrapolation of the lines in Figs. 10 and 11, since the effects of amount of carbon and age of the deposit on its activity are not accurately known, and the effects of hydrogen pressure are not the same.

REACTION MODEL

A model for the methanation reaction should be consistent with the following observations:

1. The transient tests indicate that the reaction involves competitively adsorbed species.
2. The surface is mostly covered with CO or CH_nO complexes.
3. The reaction is nearly zero order to CO over a wide range but negative order to CO at high P_{CO}. The order to CO becomes more positive at higher temperatures or higher values of P_{H_2}.
4. The order to H_2 varies between 0.5 and 1.0, increasing with P_{CO} and decreasing with P_{H_2}. The order for transient tests is lower than for steady-state tests.
5. The simple dissociation of CO is too slow to be important, but the carbon formed reacts more rapidly with H_2 than an equivalent amount of adsorbed CO.

The following mechanism is proposed with carbon as an intermediate:

$$CO_g + s \rightleftharpoons CO_s \quad (7)$$

$$(H_2)_g + s \rightleftharpoons 2H_s \quad (8)$$

$$CO_s + 2H_s \rightarrow C_s + H_2O \quad (9)$$

$$C_s + 4H_s \rightarrow CH_4 \text{ (several steps)}. \quad (10)$$

Reaction (9) involves dissociation of adsorbed CO with the participation of adsorbed H. Two atoms of hydrogen are assumed in order to account for a reaction order for H_2 up to 1.0. However, the same kinetic equation would result if CO_s reacts rapidly and reversibly with H_s to form COH_s, and this complex reacts with a second H_s to form C_s and H_2O in the slow step. Hydrogen adsorption is assumed to require only one site to make the final rate equation correspond to possible reaction orders for CO from +1 to −1. With the normal assumption that dissociative adsorption of H_2 requires two sites and reaction (9) as the slow step, the rate equation would have a limiting order of −2 for CO. At methanation conditions there are few vacant sites and very few pairs of sites, but the most negative order with respect to CO is about −1. Since H_2 molecules are small compared to CO and both are smaller than nickel atoms, one site might be sufficient for chemisorption.

If CO and H_2 in the gas phase are in equilibrium with the adsorbed species on the surface and compete for the same sites, the following equation can be derived for a uniform surface with reaction (9) as the limiting step:

$$r_{CH_4} = k\theta_{CO}\theta_H^2 = kK_{CO}K_{H_2}\frac{P_{CO}P_{H_2}}{(1 + K_{CO}P_{CO} + K_{H_2}P_{H_2})^2}, \quad (11)$$

where θ = fraction of sites covered by CO or H.

Based on Eq. (11), the steady-state reaction order with respect to H_2 is expected to be slightly less than 1.0 because of strong CO adsorption and to decrease with increasing P_{H_2}, as is shown by Fig. 2. The lower reaction order for transient studies (Fig. 7) can be explained by considering the equation for noncompetitive adsorption of H_2 once CO is no longer in the gas phase. The maximum rate in the transient tests is assumed to occur at the same value of θ_{CO} and to depend on the fraction of the remaining sites covered by H, which varies less with P_{H_2} than at steady state because the term $K_{CO}P_{CO}$ is absent:

$$r_{max} = k\theta_{CO}\theta_H^2 = k\theta_{CO}\frac{K_{H_2}P_{H_2}}{(1 + K_{H_2}P_{H_2})}(1 - \theta_{CO}). \quad (12)$$

Fitting the transient data with Eq. (12) gave a value of $K_{H_2} = 2.7$ atm^{-1} at 200°C.

Equation (11) predicts a transition from positive order for CO to negative order with increasing P_{CO}, but no one value of K_{CO} gives a good fit because of the very broad maxima in the experimental curves (Fig. 1). However, a model for a heterogeneous surface, each part of which follows Eq. (11), can give almost zero-order behavior. Evidence for heterogeneity comes from the response to a step decrease in CO, which showed the rate rising to a sharp maximum followed by a long gradual decrease. For uniform activity of the catalyst (or the adsorbed carbon species), the maximum would occur when about half of the sites had been uncovered. Fairly good agreement with the shape of these curves was obtained by assuming three types of sites, with relative activities of 1, $\frac{1}{5}$, and $\frac{1}{30}$, and 20% or less of the surface having the most active sites. This three-site model with different values of K_{CO} also gave a reasonable fit to the broad maximum in the steady-state rate curves. However, the resulting values of K_{CO} and activity for the different sites are considered only an indication of the possible heterogeneity of the catalyst and not evidence for a particular distribution.

To obtain further evidence for heterogeneity, initial rates of methanation were measured for different amounts of CO adsorbed, which were obtained by exposing the catalyst to low partial pressures of CO in He. As shown in Fig. 12, the rate was almost proportional to θ_{CO}, but the fraction of the surface covered by hydrogen was greater at low CO coverage. Assuming the rate to be proportional to θ_H^2 or to $(1 - \theta_{CO})$, the corrected rates show a large increase with θ_{CO}. The additional molecules of CO adsorbed at high P_{CO} are more weakly adsorbed but seem more active than those adsorbed at very low P_{CO}.

The reason for the heterogeneity of the catalyst surface is not known. The most active sites could be at steps on the surface

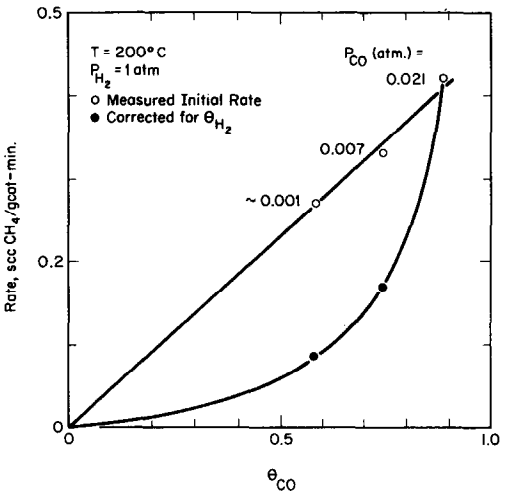

FIG. 12. Activities of adsorbed CO as a function of CO surface coverage for the 10% Ni catalyst.

or at the edges and corners where crystal faces meet. A continuous distribution of activity may result from adsorbate–adsorbate interaction. The accumulation of inactive carbon may lead to differences in activity at different sites. Further work is needed to verify the extent of heterogeneity and investigate possible causes.

REFERENCES

1. Vlasenko, V. M., and Yuzefovich, G. E., *Russ. Chem. Rev.* **38**, 728 (1969).
2. Mills, G. A., and Steffgen, F. W., *Catal. Rev. Sci. Eng.* **8**, 159 (1973).
3. Vannice, M. A., *Catal. Rev. Sci. Eng.* **14**, 153 (1976).
4. Vlasenko, V. M., Kukhar, L. A., Rusov, M. T., and Samchenko, N. P., *Kinet. Catal. USSR* **5**, 301 (1964).
5. Vlasenko, V. M., Yusotovich, G. K., and Rusov, M. T., *Kinet. Catal. USSR* **6**, 661, (1965).
6. Wedler, G., Papp, H., and Schroll, G., *J. Catal.* **38**, 153 (1975).
7. Horgan, A. M., and King, D. A., in "Adsorption–Desorption Phenomena" (F. Ricca, Ed.), p. 329. Academic Press, New York, 1972.
8. Farrauto, R. J., *J. Catal.* **41**, 482 (1976).
9. Vannice, M. A., *J. Catal.* **37**, 449, 462 (1975).
10. McGill, R. M., and Richardson, J. T., *in* "Proceedings of the 41st Annual Chemical Engineering Symposium, I & EC Division, American Chemical Society," Pittsburgh, April 1975.
11. Fontaine, R. W., and Harriott, P., *in* "Proceedings of the 41st Annual Chemical Engineering

Symposium, I & EC Division, American Chemical Society," Pittsburgh, April 1975.
12. Polizzotti, R. S., Schwarz, J. A., and Kugler, E. L., *in* "Symposium on Advances in Fischer–Tropsch Chemistry, Division of Petroleum Chemistry, American Chemical Society," Anaheim, March 1978.
13. Blyholder, G., and Neff, L. D., *J. Catal.* **2,** 138 (1961).
14. Araki, M., and Ponec, V., *J. Catal.* **44,** 439 (1976).
15. Madden, H. H., and Ertl, G., *Surface Sci.* **35,** 211 (1973).
16. McCarty, J. G., Wentrcek, P. R., and Wise, H., *in* "Symposium on Catalyst Degradation, Poisoning, Sintering and Restructuring, Petroleum Chemistry Division, American Chemical Society," Chicago, August 1977.
17. Wentrcek, P. R., Wood, B. J., and Wise, H., *J.Catal.* **43,** 363 (1976).
18. Wedler, G., Papp, H., and Schroll, G., *Surface Sci.* **44,** 463 (1974).
19. Tottrup, P. B., *J. Catal.* **42,** 29 (1976).
20. Eastman, D. E., Demuth, J. E., and Baker, J. M., *J. Vac. Sci. Technol.* **11,** 273 (1974).
21. Erley, W., and Wagner, H., *Surface Sci.* **74,** 333 (1978).